

Single-photon emission mediated by single-electron tunneling in plasmonic nanojunctions

Q. Schaefferbeke,^{1,2} R. Avriller,¹ T. Frederiksen,^{2,3} and F. Pistolesi¹

¹*Univ. Bordeaux, CNRS, LOMA, UMR 5798, F-33405 Talence, France*

²*Donostia International Physics Center (DIPC), E-20018, Donostia-San Sebastián, Spain*

³*Ikerbasque, Basque Foundation for Science, E-48013, Bilbao, Spain*

(Dated: October 31, 2019)

Recent scanning tunneling microscopy (STM) experiments reported single-molecule fluorescence induced by tunneling currents in the nanoplasmonic cavity formed by the STM tip and the substrate. The electric field of the cavity mode couples with the current-induced charge fluctuations of the molecule, allowing the excitation of photons. We investigate theoretically this system for the experimentally relevant limit of large damping rate κ for the cavity mode and arbitrary coupling strength to a single-electronic level. We find that for bias voltages close to the first inelastic threshold of photon emission, the emitted light displays anti-bunching behavior with vanishing second-order photon correlation function. At the same time, the current and the intensity of emitted light display Franck–Condon steps at multiples of the cavity frequency ω_c with a width controlled by κ rather than the temperature T . For large bias voltages, we predict strong photon bunching of the order of κ/Γ where Γ is the electronic tunneling rate. Our theory thus predicts that strong coupling to a single level allows current-driven non-classical light emission.

Electronic transport coupled to the field of an electromagnetic cavity can be realized in a wealth of different systems. This includes in the microwave range carbon-nanotubes [1–5], quantum-dots [6–9], and Josephson-junctions [10–12], or in the optical range, molecules in plasmonic nanocavities, formed by an STM tip with a substrate [13–24] and organic microcavities [25–27], or with waveguide quantum electrodynamic systems [28–30]. The reduction of the cavity volume \mathcal{V} allows to increase the zero-point quantum fluctuations of the electric field $E_{zpm} \sim \mathcal{V}^{-1/2}$. This motivated optical studies of molecular two-level systems strongly coupled to the cavity field by the dipolar interaction $\Lambda_d \sim pE_{zpm}$, (with p the molecule dipole moment). One of the goals of this effort is to reach Λ_d larger than κ , which has been and remains challenging, despite recent achievements [31]. On the other side, the coupling of a cavity mode to the current-induced charge fluctuations of a single-electronic level is given by a monopolar coupling constant $\Lambda_m \sim eLE_{zpm}$ as derived in Ref. [32] (see also [33]), with L the typical extension of the transport region and e the electronic charge. Since typically in a given system $eL \gg p$, the monopolar coupling constant is much larger than the dipolar one [32]. This probably contributed to the observation of values of Λ_m larger than κ in microwave cavities coupled to electronic transport [4, 6, 8] and even approaching the cavity resonating frequency ω_c ($\hbar = 1$) [11, 34, 35]. Recent results in plasmonic cavities coupled to electronic transport [17, 21, 22] open thus the possibility to explore transport through a single electronic level in these structures. This is expected to reach much larger coupling constants than those currently observed for purely dipolar coupling, requiring further theoretical investigations.

The system presents strong analogies with electron-

transport coupled to molecular vibrations. This has been investigated in different regimes, leading to the striking prediction of Franck–Condon blockade [36–38] and its observation [39, 40]. However, there are important differences: The first is the low quality factor of plasmonic cavities, which is typically of the order of 10 [31]. The second, and more interesting, is that the state of the optical or microwave cavity can be directly measured by detecting the emitted photons. It is thus important to investigate how transport through a molecule is linked to the property of the emitted radiation [41–43].

In this paper we consider electronic transport through a single-level quantum dot, where the charge on the dot is coupled to the electric field of an electromagnetic cavity. We propose a theoretical model to obtain the cur-

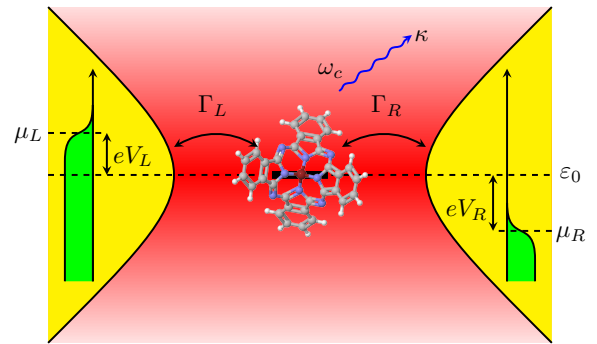


Figure 1. Schematic of two metallic electrodes forming a plasmonic nanocavity characterized by a resonating frequency $\omega_c/2\pi$ and damping rate κ . A single electronic level ε_0 of a molecule in the nanogap couples to the electromagnetic radiation with coupling constant Λ_m . Electrons can tunnel to and from the dot with tunneling rates Γ_α . Voltage drops, V_α , with respect to ε_0 are indicated.

rent through the quantum dot taking into account the cavity dissipation κ , and arbitrary values of the coupling strength in the incoherent transport regime $\Gamma \ll k_B T$, with Γ the electron tunneling rate, T the temperature, and k_B the Boltzmann constant. Similarly to the Franck-Condon case, we find current steps at the inelastic thresholds for photon emission, but with a width controlled by κ rather than T . We also derive the photon distribution and the second-order photon correlation function $g^{(2)}(t)$, where t is the emission time. Its behavior for $t = 0$ clearly shows that close to the first threshold for photon emission, for $\Gamma/\kappa \ll 1$, and $\Lambda_m \approx \omega_c$, photons anti-bunch: The junction becomes a single-photon source based on single-electron tunneling. This mechanism is different from the one assumed to be responsible for recently observed anti-bunching of emitted light in STM plasmonic nanojunctions involving multiple electronic levels [20]. For large bias voltages we find instead strong photon bunching with $g^{(2)}(0) \approx \kappa/\Gamma \gg 1$.

Model. Figure 1 shows a schematic of the system at hand. The Hamiltonian is written $H = H_S + H_I + H_B$, where

$$H_S = \tilde{\varepsilon}_0 d^\dagger d + \omega_c a^\dagger a + \Lambda_m d^\dagger d (a + a^\dagger), \quad (1)$$

with d^\dagger the creation operator for the electron on the dot single level of energy $\tilde{\varepsilon}_0$, a^\dagger the creation operator for the photon field, and $\Lambda_m = \lambda \omega_c$ the coupling constant. We follow Ref.[32] for the derivation of the interaction term [33]. We neglect direct coupling of the cavity field to the electrons in the leads, since this effect is analogous to the coupling of the cavity field to the photon bath. We treat the electrons in the leads and the propagating electromagnetic modes as a bath: $H_B = \sum_{\alpha k} \varepsilon_{\alpha k} c_{\alpha k}^\dagger c_{\alpha k} + \sum_q \omega_q b_q^\dagger b_q$, where $c_{\alpha k}^\dagger$ and b_q^\dagger are the creation operators for the electrons on the leads $\alpha = L, R$ with energy $\varepsilon_{\alpha k}$ and for the propagating photons of energy ω_q , respectively. The (linear) coupling to the bath is given by $H_I = \sum_{\alpha k} [t_{\alpha k} c_{\alpha k}^\dagger d + t_{\alpha k}^* d^\dagger c_{\alpha k}] + \sum_q [l_q a^\dagger b_q + l_q^* b_q^\dagger a]$, with $t_{\alpha k}$ and l_q the tunneling amplitudes. We first perform a standard Lang-Firsov unitary transformation on the Hamiltonian $\tilde{H} = U H U^\dagger$, with $U = e^{\lambda d^\dagger d (a - a^\dagger)}$. This removes explicitly the electron-photon coupling term in H_S , shifts the dot-level energy $\varepsilon_0 = \tilde{\varepsilon}_0 - \Lambda_m^2/\omega_c$ and modifies the d operator in H_I into $D = d e^{\lambda(a - a^\dagger)}$.

Master-equation. Let us define the reduced density matrix $\rho(t)$ for the d and a degrees of freedom after tracing out the bath. We assume that the molecule is sufficiently isolated from the substrate, as is reasonable for STM experiments performed on thin insulating films [14, 19–22].

We consider then the relevant regime $\Gamma \ll k_B T \ll \omega_c$ where the dynamics of $\rho(t)$ can be described by the Born-Markov master equation:

$$\dot{\rho}(t) = \mathcal{L}\rho(t) = -i[\tilde{H}_S, \rho(t)] + (\mathcal{L}_c + \mathcal{L}_e)\rho(t). \quad (2)$$

The first term contributing to the Liouvillian operator \mathcal{L} gives the coherent evolution of $\rho(t)$. The sec-

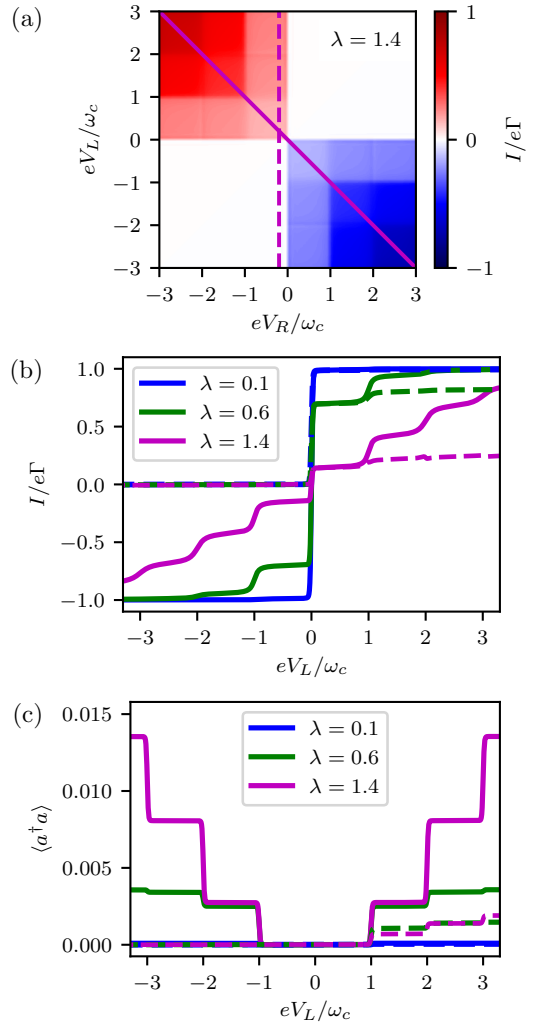


Figure 2. (a) Electronic current I versus the voltage drops V_L and V_R for $\lambda = 1.4$. (b) Current-voltage characteristics and (c) average photon occupation $\langle a^\dagger a \rangle$ in the cavity corresponding to the voltage profiles indicated in panel a (dashed and full lines) for different electron-photon coupling strengths $\lambda = 0.1$ (blue), $\lambda = 0.6$ (green) and $\lambda = 1.4$ (magenta). The model parameters are $\kappa = 10k_B T = 0.1\omega_c$ and $\Gamma_L = \Gamma_R = \Gamma/2 = 10^{-3}\omega_c$.

ond one describes the damping of the cavity mode [44, 45]: $\mathcal{L}_c \rho(t) = \kappa (2a\rho(t)a^\dagger - a^\dagger a\rho(t) - \rho(t)a^\dagger a) / 2 - \kappa n_B [a^\dagger, [a, \rho(t)]]$, with $n_B(\omega_c) = \{e^{\omega_c/k_B T} - 1\}^{-1}$ the Bose distribution of photons in the bath at the cavity frequency. The last term describes incoherent electron tunneling $\mathcal{L}_e \rho(t) = [\mathcal{D}_- \rho(t) - \rho(t)\mathcal{D}_+, D^\dagger] + \text{h.c.}$ [46], where $\mathcal{D}_\pm = \int_{-\infty}^{\infty} d\omega \int_0^{\infty} dt \Gamma_\alpha(\omega) f_\alpha^\pm(\omega) e^{i\omega t} D_I(-t)$, and $\Gamma_\alpha = 2\pi \sum_k |t_{\alpha k}|^2 \delta(\omega - \varepsilon_{\alpha k})$ is the tunneling rate from the lead α , that in the usual wide-band approximation becomes ω -independent. Finally, $D_I(-t)$ is the D operator in the interaction representation with respect to \tilde{H}_S . We introduced the short-hand notation $f_\alpha^+(\omega) = 1 - f_\alpha^-(\omega) = n_F(\omega - \mu_\alpha)$, with μ_α the chem-

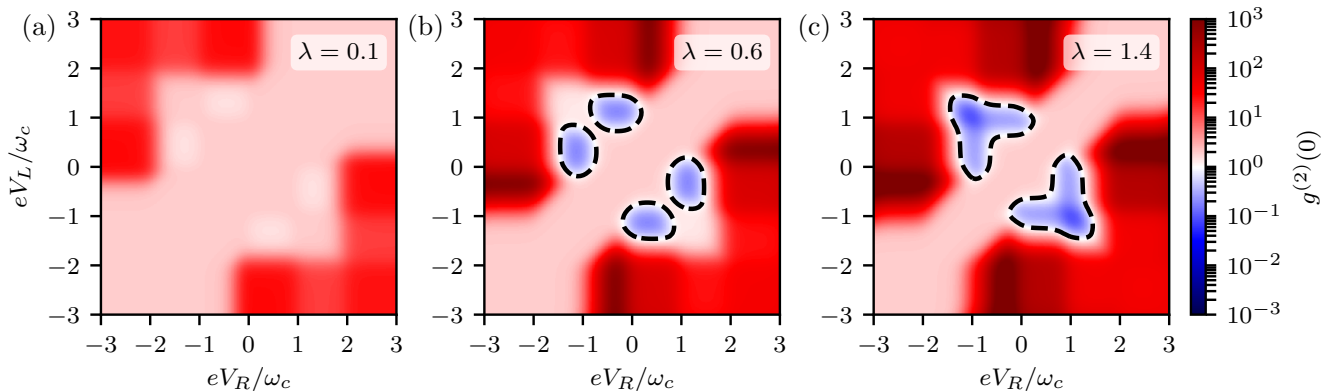


Figure 3. Degree of coherence $g^{(2)}(0)$ for different electron-photon coupling strengths (a) $\lambda = 0.1$, (b) $\lambda = 0.6$, and (c) $\lambda = 1.4$, respectively. The black dashed lines mark the contour $g^{(2)}(0) = 1$ delimiting the regions of anti-bunching (blue areas). The model parameters are $\kappa = k_B T = 0.1\omega_c$ and $\Gamma_L = \Gamma_R = 10^{-3}\omega_c$.

ical potential of lead α and $n_F(\omega) = \{e^{\omega/k_B T} + 1\}^{-1}$ the Fermi distribution. The average or the correlation function of any observable A , B , can then be calculated in the stationary regime by $\langle A \rangle = \text{Tr}[A\rho^{\text{st}}]$ and $S_{AB}(t) = \langle A(t)B(0) \rangle = \text{Tr}[Ae^{\mathcal{L}t}B\rho^{\text{st}}]$ [47, 48], with ρ^{st} the stationary solution of Eq. (2).

Electronic current. Using the previous results, we derive the expression for the average electronic dc-current evaluated at lead α

$$I_\alpha = \frac{e\Gamma_\alpha}{\pi} \text{Re} \int_{-\infty}^{\infty} d\omega \{f_\alpha^+(\omega)S_{D D^\dagger}(\omega) + f_\alpha^-(\omega)S_{D^\dagger D}(\omega)\} \quad (3)$$

where we introduced the Fourier transform of f_α^\pm , $S_{D D^\dagger}$ and $S_{D^\dagger D}$. Equation (3) enables to calculate the current in presence of strong damping rates κ , that for plasmonic cavities reaches low quality factors $\omega_c/\kappa \approx 10$ [31]. It allows to include the damping of the electromagnetic field during the tunneling process. This expression and ρ^{st} can be evaluated numerically by projecting on the charge and harmonic oscillator basis.

Figure 2(a) reports the electronic current I for strong coupling, $\lambda = 1.4$, as a function of the relative voltage drops $eV_\alpha = \mu_\alpha - \varepsilon_0$ between the chemical potential of lead α and the dot energy level [49]. Specific current-voltage characteristics, corresponding to symmetric ($V_L = -V_R$) and asymmetric ($eV_R = -0.2\omega_c$) voltage drops, are shown respectively as full and dashed lines in Fig. 2(b), for weak ($\lambda = 0.1$), moderate ($\lambda = 0.6$), and strong ($\lambda = 1.4$) coupling strengths. These exhibit similar features of the Franck-Condon blockade regime [36–38], with inelastic steps observed each time the voltage drop $eV_L = n\omega_c$ matches a multiple of the cavity-photon frequency. This is the threshold for one-electron tunneling while emitting n photons in the cavity. The step heights are given by the Poisson distribution $\mathcal{P}_n(\lambda) = e^{-\lambda} \lambda^{2n}/n!$ and the width of the inelastic steps by the cavity-losses κ , which exceed the temper-

ature broadening. This is analogous to the broadening of phonon sidebands by frictional damping [36], but our treatment is not bound to thermal equilibrium.

Emitted light. We consider now the emitted light power $\sim \kappa\omega_c \langle a^\dagger a \rangle$, by plotting the average population of the cavity mode in Fig. 2(c) as a function of V_L . We find that the photon population also increases with bias voltage in a step-like manner [50], correlated to the evolution of the electronic current [46], thus confirming that single-electron tunneling is at the origin of light-emission inside the cavity. From Eq. (2), performing a secular approximation, we derive a rate equation for the photon population $P_n(t)$ [33]. A relevant experimental regime in plasmonic cavities is $\kappa \gg \Gamma$ and $\omega_c \gg k_B T$. Since the time between two tunneling events is much longer than the damping time of the cavity, typically the circulating photon leaks out before a new photon is emitted in the cavity. In this limit $P_0 \approx 1$, and we find for the other populations $P_n = \Gamma_{0n}/n\kappa \ll 1$, with $\Gamma_{0n} = \sum_\alpha \Gamma_\alpha \mathcal{P}_n(\lambda) n_F(n\omega_c - \mu_\alpha)$ the cavity 0 to n -photons transition rate induced by a single tunneling event. The expression for $\langle a^\dagger a \rangle = \sum_n \Gamma_{0n}/\kappa$ describes then accurately the emitted power.

Correlation function $g^{(2)}$. In order to characterize the statistics of the emitted light, we compute the second-order correlation function $g^{(2)}(t) = \langle a^\dagger a^\dagger(t)a(t)a \rangle / \langle a^\dagger a \rangle^2$ [44, 51–53]. Let us begin with the $t = 0$ case, $g^{(2)}(0) = (\sum_n n(n-1)P_n) / (\sum_n nP_n)^2$. One can readily verify that in thermal equilibrium $g^{(2)}(0) = 2$. On Fig. 3 we show $g^{(2)}(0)$ as a function of V_R and V_L , for three different values of λ . As expected, for $e|V_L - V_R| \ll k_B T$, one always finds the value of 2, corresponding to thermal equilibrium (pink regions on the diagonal $V_L = V_R$). Out of equilibrium we find either bunching $g^{(2)}(0) > 1$ or anti-bunching $g^{(2)}(0) < 1$. The anti-bunching appears for sufficiently strong coupling and is indicated by the blue regions with dashed border (where $g^{(2)}(0) = 1$). Treating

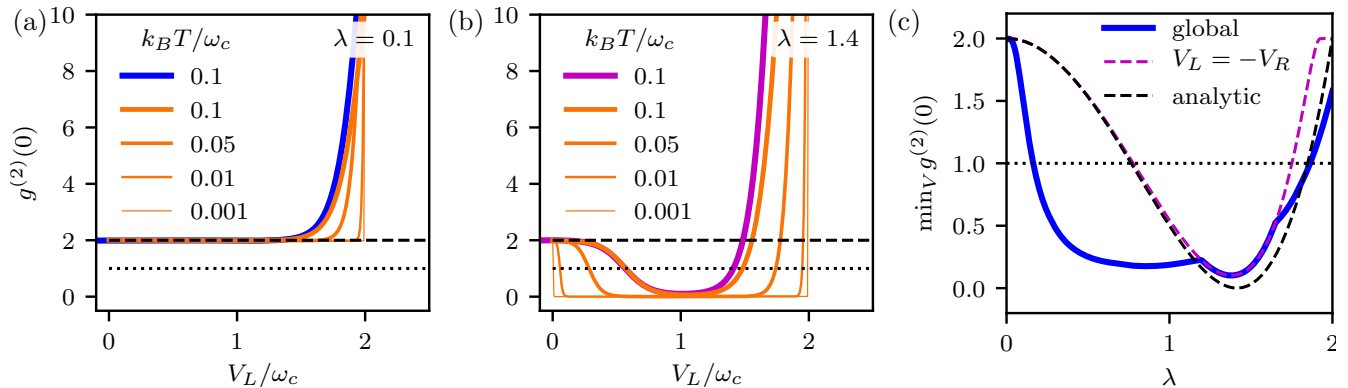


Figure 4. (a), (b) Role of temperature T on the degree of coherence $g^{(2)}(0)$ for $V_L = -V_R$ with (a) $\lambda = 0.1$ and (b) $\lambda = 1.4$. Blue and magenta thick lines are slices from Fig. 3(a,c), while the orange ones are computed from rate equations [33]. Dashed (dotted) horizontal line indicates $g^{(2)}(0) = 2$ (1) for thermal (uncorrelated) photon emission. (c) Minimum value of $g^{(2)}(0)$ on the plane (V_L, V_R) , for fixed λ and $k_B T = 0.1\omega_c$. Dashed magenta line shows that minimum constrained to $V_L = -V_R$. Dashed black line gives the $T = 0$ analytical prediction $(\lambda^2 - 2)^2/2$. Other parameters are those of Fig. 3.

both the electron tunneling and the thermal excitations as weak perturbation to the distribution $P_n = \delta_{n,0}$ we obtain an analytical expression for $g^{(2)}(0)$ (see [33]) for voltages $eV_L = -eV_R \leq 2\omega_c$.

The prediction of this expression agrees very well with the numerical calculations for $k_B T \geq 0.1\omega_c$, (cf. thick lines in Fig. 4(a) and (b)). At lower temperature we thus show only the result obtained with the analytical expression, that does not suffer from numerical instability. In the strong coupling regime, we predict a smooth crossover from the equilibrium value $g^{(2)}(0) = 2$ at low voltage, to an anti-bunching $g^{(2)}(0) < 1$ regime that appears close to the first inelastic threshold ($|eV_L| \approx \omega_c$ or $|eV_R| \approx \omega_c$) [33, 54]. As temperature decreases the region of anti-bunching expands, eventually including almost the full bias range $[0, 2\omega_c]$, cf. Fig. 4(b).

Figure 4(c) shows the minimum value taken by $g^{(2)}(0)$ when minimized on the plane (V_L, V_R) for a given value of the coupling λ . One finds that anti-bunching can be observed for $\lambda > 0.17$ for an asymmetric bias configuration, thus being at reach of present experiments. The case of symmetric bias is also shown, with anti-bunching beginning at $\lambda > 0.76$. Let us discuss now the anti-bunching mechanism for symmetric bias. When $P_{n+1} \ll P_n$, at lowest order $g^{(2)}(0) = 2P_2/P_1^2$. This expression gives 2 for thermal distribution $P_n \sim e^{-n\omega_c/k_B T}$. Anti-bunching is thus achieved for $2P_2 \ll P_1^2$. At very low temperature the only way to populate the state 2 is either a 2-photons transition (for $eV_L > 2\omega_c$), or an electron-tunneling assisted transition from the state 1 to the state 2, controlled by $\Gamma_{12} = e^{-\lambda^2} \lambda^2 (2 - \lambda^2)^2 \sum_{\alpha} \Gamma_{\alpha} n_F(\omega_c - \mu_{\alpha})/2$ (for $eV_L > \omega_c$). As a confirmation one finds that $P_1 \approx P_0 \Gamma_{01}/\kappa$ and $P_2 \approx P_1 \Gamma_{12}/2\kappa$, testifying that the result is just due to a balance between the light leaked out of the cavity and the photons emitted in the cavity

by the tunneling electrons. From the explicit expression of Γ_{12} at low temperature ($k_B T \ll \omega_c$) one then finds that the minimum value of $g^{(2)}(0)$ is approximated by $(\lambda^2 - 2)^2/2$ [dashed black line in Fig. 4(c)], tracing the λ -dependence of Γ_{12} . Its vanishing for $\lambda = \sqrt{2}$ is thus at the origin of the anti-bunching. A similar effect has also been recently reported in dc-biased Josephson junction coupled to microwave resonators [11, 12].

For larger voltages $eV_L \geq 2\omega_c$, we obtain analytically [33] $g^{(2)}(0) \approx \kappa/2\Gamma$, as predicted by the numerical simulations giving a smooth evolution to strong bunching. This result agrees with the infinite bias voltage limit result recently reported in Ref. [55]. Finally the time dependence of $g^{(2)}(t)$ as obtained by the numerical calculations shows a smooth crossover on a time scale $1/\kappa$ from $g^{(2)}(0) = 2$ to $g^{(2)}(\infty) = 1$ (uncorrelated photons) [52]. Only for $\lambda \approx 1$ we observe weak oscillations [33].

Conclusions. Charge fluctuations induced by electronic transport in a molecular *single*-electronic level are expected to couple strongly to the plasmonic mode formed by an STM tip and the substrate. We derived an expression for the current taking into account the strong damping of these cavities and obtained the current, emitted light intensity, and the correlation function $g^{(2)}(t)$. We showed that when the coupling strength is of the order $\lambda \sim 1$, Franck-Condon steps appear in both the current and the light intensity. Non-classical light can be emitted for a coupling strength in the range $0.17 < \lambda < 1.8$ for bias voltage near the one photon emission threshold. This prediction can be relevant for a series of experiments on STM cavities [16–24]. The importance of single-level descriptions has further been reinforced experimentally after our initial submission [56]. The fast evolution of the cavity ($\kappa > k_B T$) might question the validity of the Markov approximation. We esti-

mate that the non-Markovian contributions are negligible as far as $k_B T \ll \omega_c$, but investigating low-frequency response of plasmonic cavities could unravel such effects. Another interesting direction is the study of current response in presence of light irradiation of the plasmonic junction. Finally, we note that a local quantum emitter can be used to sense the environment of the molecule with the minimal quantum of energy.

Acknowledgments. We thank Tomáš Neuman, Javier Aizpurua, and Guillaume Schull for stimulating discussions. This work was supported by IDEX Bordeaux (No. ANR-10-IDEX-03-02) and Euskampus Transnational Common Laboratory *QuantumChemPhys*. T.F. acknowledges grant FIS2017-83780-P from the Spanish Ministerio de Economía y Competitividad. R.A. acknowledges financial support by the Agence Nationale de la Recherche project CERCa, ANR-18-CE30-0006.

-
- [1] M. R. Delbecq, V. Schmitt, F. D. Parmentier, N. Roch, J. J. Vienneot, G. Fève, B. Huard, C. Mora, A. Cottet, and T. Kontos, *Phys. Rev. Lett.* **107**, 256804 (2011).
- [2] L. E. Bruhat, J. J. Vienneot, M. C. Dartiailh, M. M. Desjardins, T. Kontos, and A. Cottet, *Phys. Rev. X* **6**, 021014 (2016).
- [3] A. Cottet, M. C. Dartiailh, M. M. Desjardins, T. Cubaynes, L. C. Contamin, M. Delbecq, J. J. Vienneot, L. E. Bruhat, B. Douot, and T. Kontos, *J. Phys.: Condens. Matter* **29**, 433002 (2017).
- [4] L. E. Bruhat, T. Cubaynes, J. J. Vienneot, M. C. Dartiailh, M. M. Desjardins, A. Cottet, and T. Kontos, *Phys. Rev. B* **98**, 155313 (2018).
- [5] T. Cubaynes, M. R. Delbecq, M. C. Dartiailh, R. Assouly, M. M. Desjardins, L. C. Contamin, L. E. Bruhat, Z. Leghtas, F. Mallet, A. Cottet, and T. Kontos, *npj Quantum Information* **5**, 47 (2019).
- [6] X. Mi, J. V. Cady, D. M. Zajac, P. W. Deelman, and J. R. Petta, *Science* **355**, 156 (2017).
- [7] X. Mi, J. V. Cady, D. M. Zajac, J. Stehlik, L. F. Edge, and J. R. Petta, *Appl. Phys. Lett.* **110**, 043502 (2017).
- [8] A. Stockklauser, P. Scarlino, J. V. Koski, S. Gasparinetti, C. K. Andersen, C. Reichl, W. Wegscheider, T. Ihn, K. Ensslin, and A. Wallraff, *Phys. Rev. X* **7**, 011030 (2017).
- [9] Y.-Y. Liu, K. D. Petersson, J. Stehlik, J. M. Taylor, and J. R. Petta, *Phys. Rev. Lett.* **113**, 036801 (2014).
- [10] A. Wallraff, D. I. Schuster, A. Blais, L. Frunzio, R.-S. Huang, J. Majer, S. Kumar, S. M. Girvin, and R. J. Schoelkopf, *Nature* **431**, 162 (2004).
- [11] C. Rolland, A. Peugeot, S. Dambach, M. Westig, B. Kubala, Y. Mukharsky, C. Altimiras, H. le Sueur, P. Joyez, D. Vion, P. Roche, D. Esteve, J. Ankerhold, and F. Portier, *Phys. Rev. Lett.* **122**, 186804 (2019).
- [12] A. Grimm, F. Blanchet, R. Albert, J. Leppäkangas, S. Jebari, D. Hazra, F. Gustavo, J.-L. Thomassin, E. Dupont-Ferrier, F. Portier, and M. Hofheinz, *Phys. Rev. X* **9**, 021016 (2019).
- [13] R. Berndt, J. K. Gimzewski, and P. Johansson, *Phys. Rev. Lett.* **67**, 3796 (1991).
- [14] X. H. Qiu, G. V. Nazin, and W. Ho, *Science* **299**, 542 (2003).
- [15] N. L. Schneider and R. Berndt, *Phys. Rev. B* **86**, 035445 (2012).
- [16] R. Zhang, Y. Zhang, Z. C. Dong, S. Jiang, C. Zhang, L. G. Chen, L. Zhang, Y. Liao, J. Aizpurua, Y. Luo, J. L. Yang, and J. G. Hou, *Nature* **498**, 82 (2013).
- [17] G. Reecht, F. Scheurer, V. Speisser, Y. J. Dappe, F. Mathevet, and G. Schull, *Phys. Rev. Lett.* **112**, 047403 (2014).
- [18] P. Merino, C. Große, A. Roslowska, K. Kuhnke, and K. Kern, *Nat. Commun.* **6**, 8461 (2015).
- [19] Y. Zhang, Y. Luo, Y. Zhang, Y.-J. Yu, Y.-M. Kuang, L. Zhang, Q.-S. Meng, Y. Luo, J.-L. Yang, Z.-C. Dong, and J. G. Hou, *Nature* **531**, 623 (2016).
- [20] L. Zhang, Y.-J. Yu, L.-G. Chen, Y. Luo, B. Yang, F.-F. Kong, G. Chen, Y. Zhang, Q. Zhang, Y. Luo, J.-L. Yang, Z.-C. Dong, and J. G. Hou, *Nat. Commun.* **8**, 580 (2017).
- [21] H. Imada, K. Miwa, M. Imai-Imada, S. Kawahara, K. Kimura, and Y. Kim, *Phys. Rev. Lett.* **119**, 013901 (2017).
- [22] B. Doppagne, M. C. Chong, H. Bulou, A. Boeglin, F. Scheurer, and G. Schull, *Science* **361**, 251 (2018).
- [23] M. C. Chong, N. Afshar-Imani, F. Scheurer, C. Cardoso, A. Ferretti, D. Prezzi, and G. Schull, *Nano Lett.* **18**, 175 (2018).
- [24] T. Neuman, R. Esteban, D. Casanova, F. J. Garcia-Vidal, and J. Aizpurua, *Nano Lett.* **18**, 2358 (2018).
- [25] E. Orgiu, J. George, J. A. Hutchison, E. Devaux, J. F. Dayen, B. Doudin, F. Stellacci, C. Genet, J. Schachenmayer, C. Genes, G. Pupillo, P. Samorì, and T. W. Ebbesen, *Nat. Mater.* **14**, 1123 (2015).
- [26] T. Schwartz, J. A. Hutchison, C. Genet, and T. W. Ebbesen, *Phys. Rev. Lett.* **106**, 196405 (2011).
- [27] D. Hagenmüller, J. Schachenmayer, S. Schütz, C. Genes, and G. Pupillo, *Phys. Rev. Lett.* **119**, 223601 (2017).
- [28] Z. Chen, Y. Zhou, and J.-T. Shen, *Opt. Lett.* **41**, 3313 (2016).
- [29] Z. Chen, Y. Zhou, and J.-T. Shen, *Phys. Rev. A* **96**, 053805 (2017).
- [30] Y. Zhou, Z. Chen, L. V. Wang, and J.-T. Shen, *Opt. Lett.* **44**, 475 (2019).
- [31] R. Chikkaraddy, B. de Nijs, F. Benz, S. J. Barrow, O. A. Scherman, E. Rosta, A. Demetriadou, P. Fox, O. Hess, and J. J. Baumberg, *Nature* **535**, 127 (2016).
- [32] A. Cottet, T. Kontos, and B. Douçot, *Phys. Rev. B* **91**, 205417 (2015).
- [33] See Supplemental Material at [...] for the detailed derivation of the microscopic Hamiltonian, analysis of the electronic current and derivation of analytical formulas for the second-order correlation function of the cavity plasmon field which includes [32, 37, 40, 47, 54, 57].
- [34] C. Altimiras, O. Parlavecchio, P. Joyez, D. Vion, P. Roche, D. Esteve, and F. Portier, *Appl. Phys. Lett.* **103**, 212601 (2013).
- [35] M. C. Cassidy, A. Bruno, S. Rubbert, M. Irfan, J. Kammhuber, R. N. Schouten, A. R. Akhmerov, and L. P. Kouwenhoven, *Science* **355**, 939 (2017).
- [36] S. Braig and K. Flensberg, *Phys. Rev. B* **68**, 205324 (2003).
- [37] J. Koch and F. von Oppen, *Phys. Rev. Lett.* **94**, 206804 (2005).

- [38] J. Koch, F. von Oppen, and A. V. Andreev, Phys. Rev. B **74**, 205438 (2006).
- [39] R. Leturcq, C. Stampfer, K. Inderbitzin, L. Durrer, C. Hierold, E. Mariani, M. G. Schultz, F. von Oppen, and K. Ensslin, Nat. Phys. **5**, 327 (2009).
- [40] E. Burzurí, Y. Yamamoto, M. Warnock, X. Zhong, K. Park, A. Cornia, and H. S. van der Zant, Nano Lett. **14**, 3191 (2014).
- [41] M. Galperin and A. Nitzan, Phys. Rev. Lett. **95**, 206802 (2005).
- [42] K. Kaasbjerg and A. Nitzan, Phys. Rev. Lett. **114**, 126803 (2015).
- [43] F. Xu, C. Holmqvist, G. Rastelli, and W. Belzig, Phys. Rev. B **94**, 245111 (2016).
- [44] W. H. Louisell, *Quantum statistical properties of radiation* (Wiley, 1973).
- [45] C. W. Gardiner and M. J. Collett, Phys. Rev. A **31**, 3761 (1985).
- [46] R. Avriller, B. Murr, and F. Pistolesi, Phys. Rev. B **97**, 155414 (2018).
- [47] C. Cohen-Tannoudji, J. Dupont-Roc, and G. Grynberg, *Atom-Photon Interactions: Basic Processes and Applications* (Wiley, 1998).
- [48] P. G. Kirton, A. D. Armour, M. Houzet, and F. Pistolesi, Phys. Rev. B **86**, 081305(R) (2012).
- [49] We plot the symmetrized current $I = (I_L + I_R)/2$, since for asymmetric bias voltages one observes in some cases weak non-conserving contributions.
- [50] At this level of approximation, the steps of the cavity-mode occupation appear to be broadened on the scale given by temperature instead of κ .
- [51] D. F. Walls and G. J. Milburn, *Quantum optics*, 2nd ed. (Springer Berlin, 2008).
- [52] P. R. Rice and H. J. Carmichael, IEEE J. Quantum Electronics **24**, 1351 (1988).
- [53] R. J. Glauber, Phys. Rev. **131**, 2766 (1963).
- [54] X. T. Zou and L. Mandel, Phys. Rev. A **41**, 475 (1990).
- [55] T. L. van den Berg and P. Samuelsson, Phys. Rev. B **100**, 035408 (2019).
- [56] C. C. Leon, O. Gunnarsson, D. G. de Oteyza, A. Rosawska, P. Merino, A. Grewal, K. Kuhnke, and K. Kern, arXiv:1909.08117 (2019).
- [57] F. Pistolesi and S. Labarthe, Phys. Rev. B **76**, 165317 (2007).

Supplementary Material – Single-photon emission mediated by single-electron tunneling in plasmonic nanojunction

Q. Schaefferbeke,^{1,2} R. Avriller,¹ T. Frederiksen,^{2,3} and F. Pistolesi¹

¹*Univ. Bordeaux, CNRS, LOMA, UMR 5798, F-33405 Talence, France*

²*Donostia International Physics Center (DIPC), E-20018, Donostia-San Sebastián, Spain*

³*Ikerbasque, Basque Foundation for Science, E-48013, Bilbao, Spain*

(Dated: October 31, 2019)

We provide supplementary information about the microscopic Hamiltonian describing the coupling between the plasmon mode of a STM cavity and the electronic single-level of a molecule embedded between the STM tip and the substrate. The dependence of the tunneling current across the junction with the plasmon-molecule coupling strength is analyzed, and shows analogous features to the Franck-Condon blockade regime. The second-order correlation function of the cavity plasmon field is investigated further both analytically and numerically, in the full bias-voltage range and in a regime where dissipation κ of the cavity is larger than the tunneling rate Γ .

COUPLING OF THE PLASMON MODE TO THE ELECTRONIC NANOJUNCTION

Microscopic Hamiltonian

In this section, we provide more details about the microscopic Hamiltonian describing the coupling between a STM local plasmon mode, and a single molecule embedded between the STM tip and the substrate. The form of the interaction Hamiltonian in Coulomb gauge is derived in Eq. (28) of Ref. [1], for the case of a microwave cavity mode coupled to a quantum dot connected to a single electronic reservoir. Similarly to this case, the interaction Hamiltonian between the electronic STM nanocircuit (including two electronic leads and the electronic single-level of the molecule) and the cavity plasmon mode is given by [1]

$$\hat{H}_{\text{int}} = \hat{h}_{\text{int}} (a + a^\dagger), \quad (1)$$

$$\hat{h}_{\text{int}} = \Lambda_m d^\dagger d + \sum_{\alpha k} \left\{ \gamma_{\alpha k} d^\dagger c_{\alpha k} + \gamma_{\alpha k}^* c_{\alpha k}^\dagger d + \Lambda_{\alpha k} c_{\alpha k}^\dagger c_{\alpha k} \right\}. \quad (2)$$

The first term in Eq. (2) stands for the direct (monopolar) coupling between the plasmon mode and charge fluctuations of the dot-level. The corresponding coupling strength is given by the matrix element

$$\Lambda_m = -e \int d^3r |\phi_d(\vec{r})|^2 V_\perp(\vec{r}), \quad (3)$$

with $\phi_d(\vec{r})$ the dot electronic wave function, and $V_\perp(\vec{r}) = -i\omega_c \int_{\mathcal{C}(\vec{r}_0, \vec{r})} \vec{A}(\vec{l}) \cdot d\vec{l}$ the photonic pseudo-potential [1] obtained as the work of the cavity electrical field $-i\omega_c \vec{A}(\vec{l})$ (\vec{A} is the vector potential) on a path $\mathcal{C}(\vec{r}_0, \vec{r})$ connecting any reference point \vec{r}_0 to the point \vec{r} . The second term in Eq. (2) describes modulation of the electronic tunneling from the leads to the dot induced by the photonic potential. The corresponding matrix element for this coupling

is

$$\gamma_{\alpha k} = -e \int d^3r \phi_d^*(\vec{r}) \phi_{\alpha k}(\vec{r}) V_\perp(\vec{r}), \quad (4)$$

with $\phi_{\alpha k}(\vec{r})$ the Bloch function of the metallic lead $\alpha = L, R$ with quasi-momentum k . Finally, the last term of Eq. (2) stands for the direct coupling between the electrons in the leads and the cavity plasmon mode

$$\Lambda_{\alpha k} = -e \int d^3r |\phi_{\alpha k}|^2(\vec{r}) V_\perp(\vec{r}). \quad (5)$$

Orders of magnitude

The direct (monopolar) term proportional to Λ_m (see Eq. (2)) contributes to shifting the dot-level energy by an amount $\delta\varepsilon_0 = \varepsilon_0 - \tilde{\varepsilon}_0 = -\Lambda_m^2/\hbar\omega_c$. A simple estimation of the coupling strength Λ_m is obtained when neglecting the variation of the photonic pseudo-potential on the scale of the typical extension of the molecular orbitals $\Lambda_m \sim -eV_\perp(\vec{r}_m) \approx eLE_{\text{zpm}}$, with \vec{r}_m the location of the molecule, L the typical extension of the transport region, and E_{zpm} zero-point vacuum fluctuations of the cavity electric field.

The second term proportional to $\gamma_{\alpha k}$ (see Eq. (2)) provides a contribution to the damping of the cavity $\kappa^{(2)}$, obtained at the Fermi golden rule level by $\kappa^{(2)} = 2\pi/\hbar \sum_{\alpha k} |\gamma_{\alpha k}|^2 \delta(\tilde{\varepsilon}_0 + \omega_c - \varepsilon_{\alpha k})$. Using Eq. (4), we estimate $\gamma_{\alpha k} \approx t_{\alpha k} \Lambda_m/E_F$, with E_F the typical Fermi energy of the metallic leads. This rate is thus of order $\kappa^{(2)} \approx (\Lambda_m/E_F)^2 \Gamma$. For the highest coupling strength investigated in the paper, $-\delta\varepsilon_0 \approx \Lambda_m \approx \hbar\omega_c \approx 2$ eV while $E_F \approx 5 - 10$ eV for metals, so that $\kappa^{(2)} \approx 0.04 - 0.16\Gamma \leq \Gamma \ll \kappa, -\delta\varepsilon_0$. The second term in Eq. (2) is thus negligible compared to the monopolar term and to the losses κ of the cavity.

The third and last term in Eq. (2) stands for processes (allowed by charge conservation) by which electrons in the leads directly decay to the cavity plasmon mode. We

have not included explicitly this term in the Hamiltonian written in the paper, since it is equivalent to an additional dissipation channel for the plasmon mode, already taken into account by our phenomenological damping term $\propto \kappa$.

We thus have shown that the monopolar term provides an important (even dominant) contribution to the interaction Hamiltonian in Eq. (2) describing the coupling of a single-electronic level to the cavity plasmon mode.

ELECTRONIC TUNNELING CURRENT

Photonic analogue to the Franck-Condon blockade

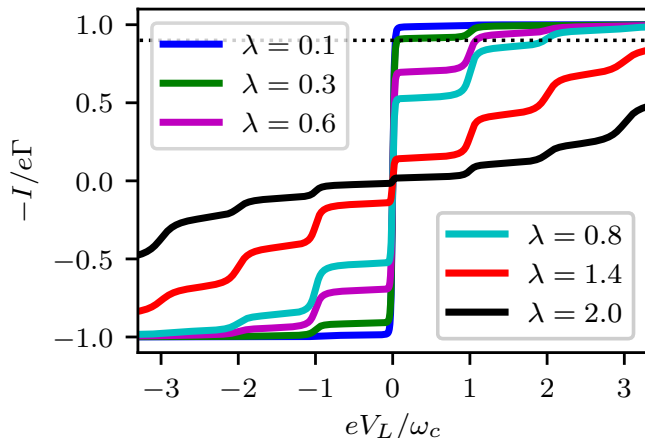


Figure S1. Current as a function of the left voltage drop eV_L for a fully symmetrical junction. $V_L = -V_R$, $\Gamma_L = \Gamma_R$, $T = 0.01\omega_c$, $\kappa = 0.1\omega_c$. The black dotted line indicates the value 0.9 corresponding to 90% of the maximum value of the current.

We present in Fig. S1 the electronic current I as a function of the voltage drop eV_L in a symmetrical junction ($V_L = -V_R$) for various values of the coupling strength λ . We show that $I(V_L)$ presents steps each times the voltage drop reaches a n -photon emission threshold $V_L \approx n\omega_c$. The height of those steps increases with λ and after reaching a maximum, decreases again. Furthermore, Fig. S1 shows that as λ increases, the current gets blocked at low voltages, a phenomenon sharing strong analogies to the Franck-Condon blockade regime observed in molecular junctions with phonons [2, 3].

We present in Fig. S2 the evolution of the electronic current I at low-voltage $eV_L = 0.5\omega_c$ with coupling strength λ . Using Franck-Condon blockade theory at low temperature ($T \ll \omega_c$) and in the equilibrated regime for the photon population [2], we expect the current to scale as

$$I \approx \Gamma e^{-\lambda^2} \sum_{n=0}^{+\infty} \frac{\lambda^{2n}}{n!} n_F(n\omega_c - V_\alpha). \quad (6)$$

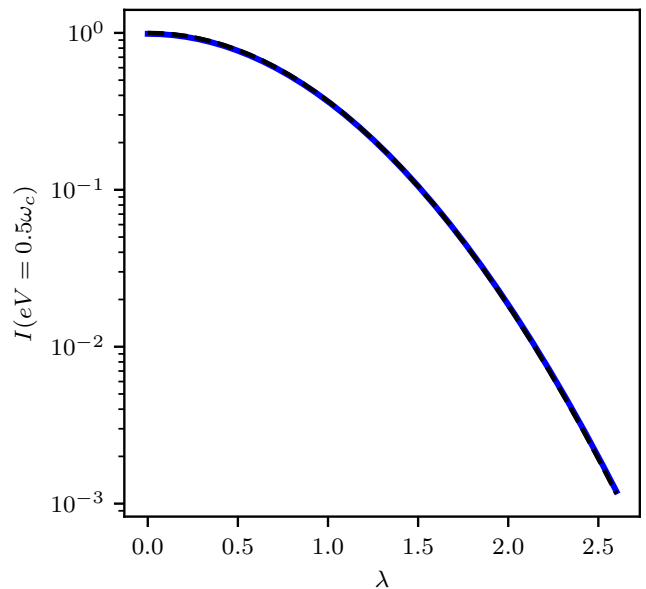


Figure S2. Plain blue curve: Value of the current I at $eV_L = 0.5\omega_c$ as a function of the coupling strength λ in the case of a fully symmetric junction ($V_L = -V_R = V$, $\Gamma_L = \Gamma_R = 0.001\omega_c$ and $k_B T = 0.01\omega_c$). In dashed black is represented the expected dependence $\ln(I/\Gamma) \approx -\lambda^2$ provided by Eq. (6).

Clearly, while Eq. (6) properly predicts the appearance of inelastic thresholds in the current $I(V_L)$, when $V_\alpha \approx n\omega_c$. It also predicts a width of the steps that is proportional to temperature T , in contrast to Fig. S1 which exhibits steps with a width given by the dissipation rate of the cavity κ . This is clearly due to the fact that Eq. (6) does not properly include a description of cavity losses.

However, some qualitative features present in Fig. S1 are preserved by Eq. (6). For instance, for voltages below the first inelastic threshold $V_L < \omega_c$, Eq. (6) predicts an exponential suppression of the low-bias current: $\ln(I/\Gamma) \approx -\lambda^2$, which is indeed obtained in Fig. S2. Also, Eq. (6) predicts that the typical size of the first inelastic step $\Delta I = I(V_L = \omega_c + \eta_V) - I(V_L = \omega_c - \eta_V)$, with η_V a voltage of order κ , scales as $\Delta I \approx \Gamma \lambda^2 e^{-\lambda^2}$, thus reaching a maximum value for $\lambda \approx 1$, which is consistent with the curves of Fig. S1.

To show further the impact of λ on the current suppression, we plot in Fig. S3 the voltage drop V_{90} needed to recover 90% of the maximum current as a function of λ . Fig. S3 shows that V_{90} increases with λ in a parabolic manner: the higher λ , the stronger the current suppression at low-voltage, and the higher the needed voltage to reach saturation. It is interesting to notice that the classical analogue to Franck-Condon blockade theory [4] predicts that a critical voltage $2\omega_c \lambda^2$ is needed to unblock the junction, which scales accordingly to V_{90} in Fig. S3.

Expression of the dc-tunneling current

The current operator across lead $\alpha = L, R$ is obtained from the continuity equation for tunneling charges as

$$I_\alpha = ie \sum_k \left(t_{\alpha k} c_{\alpha k}^\dagger D - t_{\alpha k}^* D^\dagger c_{\alpha k} \right), \quad (7)$$

with e the elementary charge. The average current at time t is computed using the density matrix $\underline{\rho}(t)$ of the full system, including the molecular junction with its electronic reservoirs, and the cavity mode with the external photon bath

$$\langle I_\alpha(t) \rangle = \text{Tr} (I_\alpha \underline{\rho}(t)). \quad (8)$$

The full density matrix in Eq. (8) evolves in time with respect to the full Hamiltonian \tilde{H} (after the Lang-Firsov transformation has been performed) as

$$\dot{\underline{\rho}}(t) = -i \left[\tilde{H}, \underline{\rho}(t) \right], \quad (9)$$

$$\underline{\rho}(0) = \rho_L \otimes \rho_R \otimes \rho_b \otimes \rho(0). \quad (10)$$

The initial condition for the density matrix in Eq. (10) is chosen to be the product of density matrices of the electronic ($\rho_{\alpha=L,R}$) and bosonic (ρ_b) environments each supposed to be at equilibrium, times the initial reduced density matrix $\rho(0)$ of system (dot plus cavity-mode). We further define the "bare" Hamiltonian $H_0 = \tilde{H}_S + \tilde{H}_B = \tilde{H} - \tilde{H}_I$ containing the system and baths Hamiltonians. The "perturbation Hamiltonian" $V = \tilde{H}_I$ contains the tunneling Hamiltonian (dressed by photons) and the dissipative coupling between the cavity-mode and the photon bath. Integrating Eq. (9) with initial condition Eq. (10), we get an exact expression for the average current

$$\langle I_\alpha(t) \rangle = \text{Tr} (I_\alpha(t) \underline{\rho}(0)) - i \int_{t_0}^t dt' \text{Tr} (I_\alpha(t) [V(t'), \underline{\rho}(t')]), \quad (11)$$

with all operators written in interaction picture with respect to H_0 .

We further perform the Born approximation $\underline{\rho}(t') \approx \rho_L \otimes \rho_R \otimes \rho_b \otimes \rho(t')$ and truncate consistently Eq. (11) at lowest non-vanishing order in the tunneling rates Γ_α . We note that the first term in Eq. (11) vanishes due to our choice of initial conditions. We further expand the second term after injecting the expression of the interaction Hamiltonian V written in the paper. After coming back to Schrödinger representation, a subsequent Markov approximation enables to neglect the time dependence of $\rho(t') \approx \rho(t)$ in the time integral, and to take the limit $t_0 \rightarrow -\infty$. We obtain the final expression for the average dc-current $\langle I_\alpha \rangle = \lim_{t \rightarrow +\infty} \langle I_\alpha(t) \rangle$

$$\langle I_\alpha \rangle = \frac{e\Gamma}{\pi} \text{Re} \int_{-\infty}^{+\infty} d\omega \int_0^{+\infty} d\tau \left\{ f_\alpha^+(\omega) \langle D(\tau) D^\dagger \rangle_0 e^{i\omega\tau} - f_\alpha^-(\omega) \langle D^\dagger(\tau) D \rangle_0 e^{-i\omega\tau} \right\}, \quad (12)$$

with $\langle A(\tau) B \rangle_0 = \text{Tr} [e^{iH_0\tau} A e^{-iH_0\tau} B \rho^{st}]$ the average value of the system operators $A(\tau)$ and $B(0)$ written in interaction representation, using as initial condition the stationary density matrix $\underline{\rho}(0) \equiv \rho^{st}$.

In order to incorporate the contribution of cavity dissipation to the time evolution of the D and D^\dagger operators in Eq. (12), we further replace each term of the form $\langle A(\tau) B \rangle_0$ by the correlation function $S_{AB}(\tau) = \text{Tr} [e^{i\tilde{H}\tau} A e^{-i\tilde{H}\tau} B \rho^{st}] \equiv \text{Tr}_S [A e^{\mathcal{L}\tau} B \rho^{st}]$. *This ansatz is strictly speaking beyond Born approximation, being all orders in the damping rate κ .* Equation (3) in the main text of our paper follows after Fourier transformation of the correlation functions $S_{DD^\dagger}(\tau)$ and $S_{D^\dagger D}(\tau)$.

ANALYTICAL CALCULATION OF $g^{(2)}(0)$

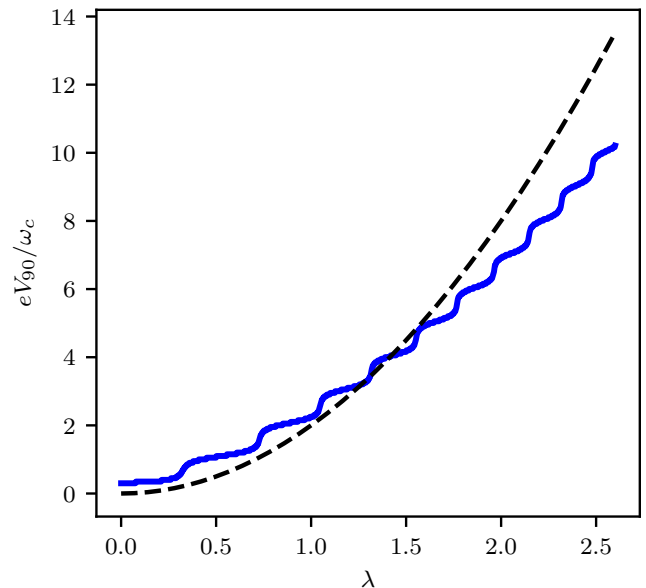


Figure S3. Value of V for which 90% of the maximum current is achieved as a function of the coupling strength λ in the case of a fully symmetric junction ($V_L = -V_R = V$, $\Gamma_L = \Gamma_R = 0.001\omega_c$ and $k_B T = 0.01\omega_c$). In dashed black, expected classical value $V_{90} = 2\omega_c\lambda^2$ at which the junction gets unblocked.

Rate equation for $P_n(t)$

We derive in this section the rate equation for the photon population $P_n(t) = \sum_{q=0,1} \Pi_{qn}(t)$, with Π_{qn} the probability of occupation of the state with $q = 0, 1$ charge on the dot and $n \in \mathbb{N}$ photons of the cavity mode. We

obtain the following rate equation for $\Pi_{qn}(t)$

$$\begin{aligned} \dot{\Pi}_{qn} = & \sum_{m=0}^{\infty} [\Gamma_{(\bar{q}m)(qn)} \Pi_{\bar{q}m} - \Gamma_{(qn)(\bar{q}m)} \Pi_{qn}] \\ & + n\kappa_{\uparrow} \Pi_{qn-1} + (n+1)\kappa_{\downarrow} \Pi_{qn+1} \\ & - [(n+1)\kappa_{\uparrow} + n\kappa_{\downarrow}] \Pi_{qn}, \end{aligned} \quad (13)$$

with $\bar{q} = 1, 0$ when $q = 0, 1$, $\kappa_{\uparrow} = \kappa n_B(\omega_c)$, and $\kappa_{\downarrow} = \kappa[1+n_B(\omega_c)]$. The transition rates $\Gamma_{(qn)(\bar{q}m)}$ involving photon emission or absorption mediated by electron tunneling events are given by Fermi golden rule

$$\Gamma_{(0n)(1m)} = \Gamma |M_{mn}|^2 \sum_{\alpha} n_F((m-n)\omega_c - V_{\alpha}) \quad (14)$$

$$\Gamma_{(1n)(0m)} = \Gamma |M_{nm}|^2 \sum_{\alpha} [1 - n_F((n-m)\omega_c - V_{\alpha})], \quad (15)$$

and $|M_{mn}|^2$ is the Franck-Condon matrix element [2] for the considered transition.

The stationary solution $P_n^{st} = \lim_{t \rightarrow +\infty} P_n(t)$ of Eq. (13) enables to calculate the second order correlation function of the cavity mode at equal time

$$g^{(2)}(0) = \frac{\langle n^2 \rangle - \langle n \rangle^2}{\langle n \rangle^2}, \quad (16)$$

with $\langle n^k \rangle \equiv \sum_{n=0}^{+\infty} P_n^{st} n^k$. In the following, we focus on the case of symmetric bias voltage $V_L = -V_R = V/2$, such that $\Gamma_{(0n)(1m)} = \Gamma_{(1n)(0m)} \equiv \Gamma_{nm}$. A simpler and closed rate equation can be derived in this case for the photon population $P_n(t)$, after integrating out the charge degree of freedom of the dot

$$\begin{aligned} \dot{P}_n = & \sum_{m=0}^{\infty} [\Gamma_{mn} P_m - \Gamma_{nm} P_n] \\ & + n\kappa_{\uparrow} P_{n-1} + (n+1)\kappa_{\downarrow} P_{n+1} \\ & - [(n+1)\kappa_{\uparrow} + n\kappa_{\downarrow}] P_n. \end{aligned} \quad (17)$$

Large bias voltage limit $V_L \geq 2\omega_c$

From now, we focus on the regime $\kappa \gg \Gamma$, for which the cavity damping rate dominates over the dissipation rate induced by tunneling electrons. We also consider low-temperatures $T = 0.1\omega_c$, such that $\kappa_{\uparrow} \ll \kappa_{\downarrow} \approx \kappa$. In this regime, the cavity is thus always close to its quantum ground state, namely $P_0 \approx 1 \gg P_{n \geq 1}$.

For $V_L \geq 2\omega_c$, we keep in Eq. (17) the leading orders in the photon populations and rates, such that

$$\dot{P}_n \approx \Gamma_{0n} P_0 + \kappa [(n+1)P_{n+1} - nP_n]. \quad (18)$$

Eq. (18) can be solved exactly leading to the stationary population

$$P_{n \geq 1}^{st} = \frac{P_0^{st}}{\kappa n} \sum_{k \geq n} \Gamma_{0k}. \quad (19)$$

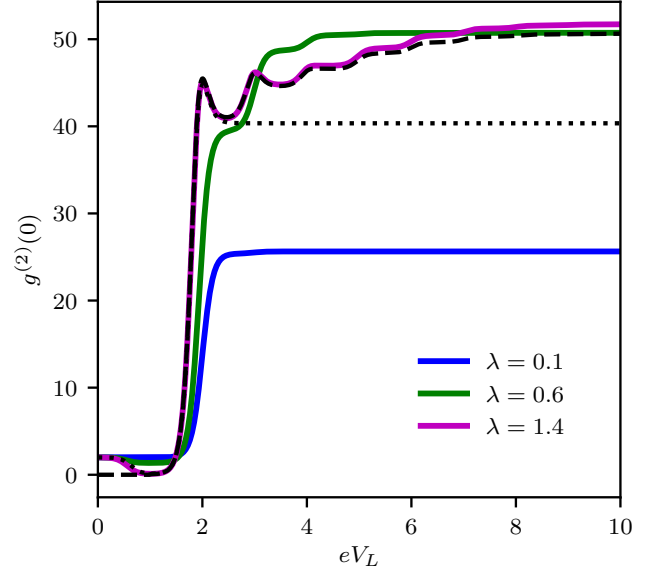


Figure S4. Degree of coherence $g^{(2)}(0)$ at time $t = 0$ as a function of the left voltage drop eV_L for three different values of the coupling strength λ . For all three curves, $k_B T = \kappa = 0.1\omega_c$ and $\Gamma_L = \Gamma_R = 0.001\omega_c$. The black dotted curve shows the analytical prediction at low bias voltage and the black dashed line shows the analytical prediction at large bias voltage for $\lambda = 1.4$ (magenta).

Incorporating Eq. (19) into Eq. (16) enables to derive an analytical expression for $g^{(2)}(0)$ that is valid at finite voltage, down to the two-photon emission threshold $V_L \geq 2\omega_c$. At the second inelastic threshold $V_L \approx 2\omega_c$, emission of photon pairs at equal time is strongly enhanced, thus resulting into a strong bunching of the $g^{(2)}(0)$ versus V curve (see black dashed curve in Fig.S4).

The infinite bias voltage limit $V \gg \omega_c$ simplifies further in Eq. (19) to

$$P_{n \geq 1}^{st} \approx P_0^{st} \frac{\Gamma}{\kappa n}, \quad (20)$$

such that

$$g^{(2)}(0) \approx \frac{\kappa}{2\Gamma}. \quad (21)$$

We thus predict a saturation of $g^{(2)}(0)$ at large voltages to a value $g^{(2)}(0) \gg 1$, corresponding to strong bunching of the emitted light. For the parameters of Fig.3 in the paper, $\Gamma \approx 10^{-3}\omega_c$ and $\kappa \approx 0.1\omega_c$, such that $g^{(2)}(0) \approx 50$, as observed in Fig.S4.

Low-voltage limit $V_L \leq 2\omega_c$

In the range of voltages $V_L \leq 2\omega_c$, we have to be more careful about how to keep the leading terms in Eq. (17), in particular in order that P_n^{st} converges to thermal equilibrium at $V_L = 0$. We found that below the two-photon

inelastic threshold ($V_L \leq 2\omega_c$), it is sufficient to keep only states involving at most 2 photons, such that Eq. (17) can be truncated and simplified as

$$\dot{P}_2 \approx \Gamma_{02}P_0 + (2\kappa_\uparrow + \Gamma_{12})P_1 - 2\kappa_\downarrow P_2 \quad (22)$$

$$\dot{P}_0 \approx \kappa_\downarrow P_1 - (\kappa_\uparrow + \Gamma_{01} + \Gamma_{02})P_0 \quad (23)$$

$$P_1 = 1 - P_0 - P_2. \quad (24)$$

The stationary solution of this system of equations provides

$$g^{(2)}(0) \approx \frac{\Delta [\kappa_\downarrow \Gamma_{02} + (2\kappa_\uparrow + \Gamma_{12})(\kappa_\uparrow + \Gamma_{01} + \Gamma_{02})]}{2[(\kappa_\uparrow + \Gamma_{01} + \Gamma_{02})(\kappa_\downarrow + 2\kappa_\uparrow + \Gamma_{12}) + \kappa_\downarrow \Gamma_{02}]^2} \quad (25)$$

with

$$\Gamma_{0n} = e^{-\lambda^2} \frac{\lambda^{2n}}{n!} \sum_{\alpha} \Gamma_{\alpha} n_F(n\omega_c - V_{\alpha}), \quad (26)$$

the rate for the transition from 0 to n photons in the cavity,

$$\Gamma_{12} = e^{-\lambda^2} \lambda^2 \frac{(2 - \lambda^2)^2}{2} \sum_{\alpha} \Gamma_{\alpha} n_F(\omega_c - V_{\alpha}), \quad (27)$$

the corresponding rate for the transition from 1 to 2 photons in the cavity, and $\Delta = (\kappa_\uparrow + \Gamma_{01} + \Gamma_{02}) [2(\kappa_\downarrow + \kappa_\uparrow) + \Gamma_{12}] + \kappa_\downarrow (2\kappa_\downarrow + \Gamma_{02})$.

Close to the one-photon inelastic threshold ($V_L \approx \omega_c$), we find that Eq. (25) predicts a minimum value for $g^{(2)}(0)$ given by $\min g^{(2)}(0) \approx \Gamma_{12}/\Gamma_{01} \approx (2 - \lambda^2)^2/2$. Eq. (25) compares well with the numerics as shown in Fig.S4 (see black dotted curve).

TIME DEPENDENCE OF $g^{(2)}(t)$

In this section, we are interested in the full time dependence of the second order correlation function $g^{(2)}(t)$ of the plasmonic field

$$g^{(2)}(t) = \frac{\langle a^\dagger a^\dagger(t) a(t) a \rangle}{\langle a^\dagger a \rangle^2} \equiv \frac{\langle a^{\dagger 2} e^{\mathcal{L}t} a^2 \rangle}{\langle a^\dagger a \rangle^2}. \quad (28)$$

$g^{(2)}(t)$ is then computed numerically using the second part of the equation, that is an expression of quantum regression theorem [5]. The curves $g^{(2)}(t)$ are shown in Fig. S5 for various values of λ , at a fixed value of bias voltage close to the first photon-emission threshold $V_L = -V_R = 1.2\omega_c$. In the limit of vanishing plasmon-molecule coupling $\lambda \rightarrow 0$, the plasmon mode gets to thermal equilibrium with the external electromagnetic bath. For a damped electromagnetic cavity at thermal equilibrium, we obtain

$$g^{(2)}(t) = \frac{\langle a^{\dagger 2} a^2 \rangle e^{-\kappa t} + n_B(\omega_c) \langle a^\dagger a \rangle [1 - e^{-\kappa t}]}{\langle a^\dagger a \rangle^2}, \quad (29)$$

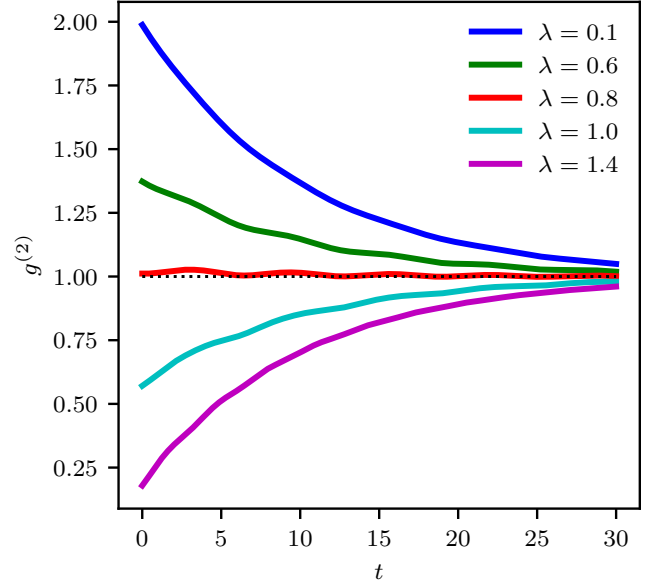


Figure S5. Degree of coherence $g^{(2)}(t)$ as a function of time t for three different values of the coupling strength λ . For all three curves, $k_B T = \kappa = 0.1\omega_c$, $\Gamma_L = \Gamma_R = 0.001\omega_c$ and $V_L = -V_R = 1.2\omega_c$. The black dotted line is at $g^{(2)} = 1$.

with an exponential decay given by κ the damping rate of the cavity. The curve $g^{(2)}(t)$ decays from $g^{(2)}(0) = 2$ its value at thermal equilibrium, to a value $g^{(2)}(t \rightarrow +\infty) = 1$ characterizing uncorrelated photon emission events at large times. Note that in this case, since $g^{(2)}(t) < g^{(2)}(0)$ close to $t = 0$, the probability of emission of two photons at the same initial time is higher than the one of emitting two successive photons, thus characterizing bunching of the emitted light. The fact that $g^{(2)}(t) > 1$ for all times means that the statistics of emitted light is super-Poissonian. As expected, the obtained blue curve ($\lambda = 0.1$) in Fig. S5 is close to the one predicted by Eq. (29).

Upon increasing λ , however, we notice a crossover towards a different regime (see magenta curve for $\lambda = 1.4$ in Fig. S5) for which, $g^{(2)}(t) > g^{(2)}(0)$ close to $t = 0$, namely the probability of emitting two photons at successive times is higher than the one of emitting two photons at the same time. *This unambiguously characterizes photon antibunching of the emitted light [6]*. Moreover, upon decreasing temperature, antibunching gets almost perfect $g^{(2)}(0) \approx 0 < 1$. The fact that $g^{(2)}(t) < 1$ at any times is a signature that the emitted light has a sub-Poissonian statistics. In the intermediate coupling regime $\lambda \approx 0.8$ (red curve in Fig. S5), $g^{(2)}(t)$ oscillates weakly in time around 1. The statistics of emitted light is thus close to the Poisson distribution obtained for a coherent classic field. We note that after checking the behavior of the full time dependence encoded in $g^{(2)}(t)$ (see Fig.S5), the knowledge of $g^{(2)}(0)$ is sufficient in Fig.S5 to characterize the existence of a crossover from a regime of

bunching ($g^{(2)}(0) > 1$) to antibunching ($g^{(2)}(0) < 1$) of photon-emission.

-
- [1] A. Cottet, T. Kontos, and B. Douçot, Phys. Rev. B **91**, 205417 (2015).
- [2] J. Koch and F. von Oppen, Phys. Rev. Lett. **94**, 206804 (2005).
- [3] E. Burzurí, Y. Yamamoto, M. Warnock, X. Zhong, K. Park, A. Cornia, and H. S. van der Zant, Nano Lett. **14**, 3191 (2014).
- [4] F. Pistolesi and S. Labarthe, Phys. Rev. B **76**, 165317 (2007).
- [5] C. Cohen-Tannoudji, J. Dupont-Roc, and G. Grynberg, *Atom-Photon Interactions: Basic Processes and Applications* (Wiley, 1998).
- [6] X. T. Zou and L. Mandel, Phys. Rev. A **41**, 475 (1990).